J. Fluid Mech. (2005), *vol.* 525, *pp.* 105–113. © 2005 Cambridge University Press
DOI: 10.1017/S0022112004002630 Printed in the United Kingdom

Asymptotic spike evolution in Rayleigh–Taylor instability

By PAUL CLAVIN[1] AND FORMAN WILLIAMS[2]

[1]Institut de Recherche sur les Phénomènes Hors Équilibre, CNRS/Université d'Aix-Marseille I & II, 49, rue Joliot Curie, BP 146, F-13384 Marseille cedex, France

[2]Center for Energy Research, Department of Mechanical and Aerospace Engineering, University of California San Diego, La Jolla, CA 92013-0411, USA

(Received 2 September 2004 and in revised form 4 November 2004)

An analytical study of the asymptotic behaviour of descending spikes is carried out for the idealized limit of an inviscid, incompressible fluid without surface tension, bounded by a vacuum. A self-similar solution is obtained for the shape of the free surface at the spike tip, yielding the evolution in time of the surface curvature there. The approach to free-fall acceleration is shown to follow an inverse power law in time. Results are given for both planar (two-dimensional) and axisymmetric spikes. Potential areas of application include ablation-front dynamics in inertial-confinement fusion.

1. Introduction

Despite a long series of impressive studies, described, for example, in the reviews of Kull (1991) and of Inogamov (1999), numerous questions concerning Rayleigh–Taylor instability remain unanswered. This is true even for the basic limit of an inviscid, incompressible fluid above a vacuum, with a tensionless interface at zero pressure. In that limit, there are solutions in which nonlinear growth of the initial instability results in the unsteady, periodic, symmetric pattern illustrated in figure 1. Bubbles, rising at an almost constant velocity, are separated by downward-moving spikes (also called fingers or jets) descending at a nearly constant acceleration, approaching that of free fall under the imposed external force. The dynamics of a single bubble is relatively well understood, thanks to the pioneering work of Rayleigh (1900), Taylor (1950) and Layzer (1955), based on a single-mode approximation of the flow at its tip, and to the more recent studies of Abarzhi (1998), Mikaelian (1998), Zhang (1998), Goncharov (2002) and Abarzhi, Nishihihara & Glimm (2003). Much less is known about the spikes, for which the dynamical system obtained with a single-mode approximation does not provide an accurate framework for describing the asymptotic dynamics (Inogamov 1999, p. 84). It is an open question as to whether finite-time singularities, dependent on the initial conditions, develop at or near the tip of the spike – a question recently addressed by conformal mapping, an approach used by Tanveer (1993) and Yoshikawa & Balk (2003), and references quoted therein.

The present paper offers a local asymptotic analysis of the spikes, based on hypotheses of regularity and small departures from free fall, intended to provide a framework for future computational and experimental tests. The computational tests can be performed by accurate numerical methods, such as integral methods (L. Duchemin & C. Josserand 2004, personal communication) and vortex-blob methods (Baker & Beale 2004). A motivation arises from interest in instabilities of ablation fronts in the

https://doi.org/10.1017/S0022112004002630 Published online by Cambridge University Press

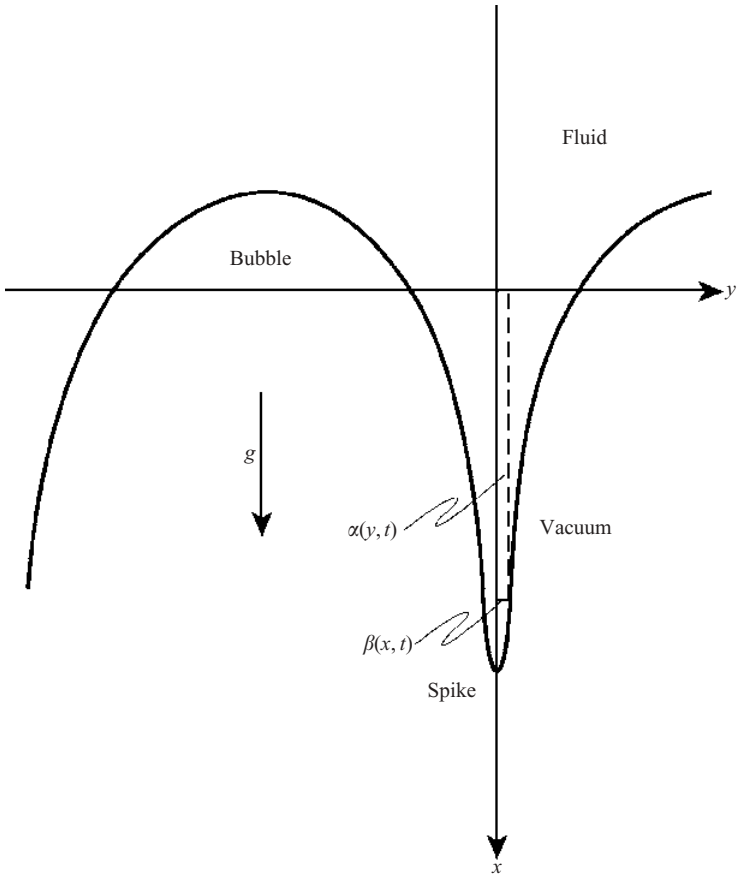


FIGURE 1. Schematic diagram of the model.

limits of small ablation velocity and large density ratio (see Appendix A). Although weak in comparison with Rayleigh–Taylor instability, ablation is expected to have a large effect on the thin elongated spikes. A preliminary step is thus to know in sufficient detail what is the asymptotic behaviour of the spikes in the idealized model without ablation. This is the purpose of the present analytical study, the result of which cannot immediately be generalized to the ablation problem but instead can provide background understanding that could be helpful in addressing the ablation problem.

The problem is formulated in § 2. The basic approximation and the perturbation methods are then presented in § 3, and the long-time asymptotic behaviour of the curvature at the tip of the spike is derived in § 4, including a self-similar solution for the equation of the free surface near the tip. Arguments are also presented here against the formation of singularities for most initial conditions. The way that the free-fall acceleration is approached is presented § 5, and § 6 is devoted to a short discussion of the results.

2. Formulation

The planar, two-dimensional coordinate system is illustrated in figure 1. The constant gravitational acceleration, of magnitude g, is directed downward, in the positive

https://doi.org/10.1017/S0022112004002630 Published online by Cambridge University Press

x-direction. The origin of the transverse coordinate y in the inertial frame is placed along a vertical line that passes through the tip of a spike, so that the interface and the flow field are symmetrical in y. The axisymmetric spike may be addressed similarly, replacing y by the radius. The fluid, inviscid and with zero surface tension, is taken to be incompressible (an approximation of low Mach number), of density ρ, with x and y velocity components u and v, respectively. If p denotes the pressure divided by ρ, then the Euler equations for an irrotational flow can be written as

$$\frac{\partial}{\partial x}u + \frac{\partial}{\partial y}v = 0, \tag{2.1}$$

$$\frac{\partial}{\partial t}u = -\frac{\partial}{\partial x}[p - gx + (u^2 + v^2)/2], \tag{2.2}$$

$$\frac{\partial}{\partial t}v = -\frac{\partial}{\partial y}[p - gx + (u^2 + v^2)/2]. \tag{2.3}$$

Since the irrotational flow is potential, the velocity vector can be expressed as

$$(u, v) = -\nabla\Phi \tag{2.4}$$

with $\nabla^2\Phi = 0$. The Bernoulli equation is then

$$\partial\Phi/\partial t = p - gx + (u^2 + v^2)/2 + C(t), \tag{2.5}$$

where $C(t)$ is a function of time.

The problem is a free-boundary problem, with the fluid occupying the region $x \leqslant \alpha(y, t)$, where the equation defining the location of the free surface is $x = \alpha(y, t)$. Initial conditions must be given if a unique solution is to be determined, and the boundary conditions far from the interface are taken to be that the fluid is at rest at infinity,

$$u = \partial\Phi/\partial x \to 0 \quad \text{and} \quad v = \partial\Phi/\partial y \to 0 \quad \text{as} \quad x \to -\infty. \tag{2.6}$$

The zero-pressure boundary condition ($p = 0$) at the interface, $x = \alpha(y, t)$, yields

$$\partial\Phi/\partial t|_{x=\alpha} = -g\alpha + (u^2|_{x=\alpha} + v^2|_{x=\alpha})/2 + C(t), \tag{2.7}$$

from (2.5). There is, in addition, a kinematic condition at the interface, stating that the boundary is moving with the fluid, namely,

$$\partial\alpha/\partial t = u|_{x=\alpha} - v|_{x=\alpha}\partial\alpha/\partial y. \tag{2.8}$$

3. Basic assumptions and perturbation method

It is assumed that the asymptotic flow at long time near the spikes corresponds to approximately steady, parallel free fall, so that

$$u\partial u/\partial x \approx g, \tag{3.1}$$

leading to

$$u \approx \sqrt{2gx}, \tag{3.2}$$

valid near the tip of the spike. The position of the tip is then described approximately by

$$x \equiv x_s(t) \approx gt^2/2, \tag{3.3}$$

https://doi.org/10.1017/S0022112004002630 Published online by Cambridge University Press

for a suitable choice of the origin of time and space. The general expression for the vertically downward component of velocity is written as

$$u = \sqrt{2(gx + f)}, \tag{3.4}$$

and the perturbation analysis will be based on the assumptions

$$|f(x, y, t)| \ll gx, \quad |\partial f(x, y, t)/\partial x| \ll g, \quad |\partial f(x, y, t)/\partial t| \ll ug, \tag{3.5}$$

to be verified *a posteriori* for self-consistency in a later section. In addition, the flow has been taken to be irrotational, and the perturbation f will be assumed to be analytic. The time-dependent ratio $|f(x_s, 0, t)|/(gx_s)$ can be viewed as the small parameter of expansion of the perturbation analysis. The analysis is carried only to first order in this parameter, which is small at long time.

4. Leading order for the spike asymptotics

The incompressibility condition may be applied to the spike in figure 1 with its tip at $y = 0$. Equations (2.1) and (3.2) thereby give

$$-\partial v/\partial y = \partial u/\partial x \approx \frac{\sqrt{g/2}}{x^{1/2}}. \tag{4.1}$$

In view of the symmetry boundary condition that $v = 0$ at $y = 0$, it follows from (4.1) that

$$v \approx -\sqrt{g/2}\frac{y}{x^{1/2}}. \tag{4.2}$$

At the leading order, (2.8), (3.2) and (4.2) provide an equation for the free interface, namely

$$\frac{1}{\sqrt{2g}}\frac{\partial}{\partial t}\alpha = \alpha^{1/2} + \frac{1}{2\alpha^{1/2}}\left(y\frac{\partial}{\partial y}\alpha\right), \tag{4.3}$$

which may be written, after dividing by $\alpha^{1/2}$, as

$$\sqrt{\frac{2}{g}}\frac{\partial \alpha^{1/2}}{\partial t} = 1 + \frac{y}{\alpha^{1/2}}\frac{\partial \alpha^{1/2}}{\partial y}. \tag{4.4}$$

It is convenient to introduce the function

$$z(y, t) \equiv t - \alpha^{1/2}\sqrt{(2/g)}, \tag{4.5}$$

which is, by definition, a function increasing with $|y|$, satisfying $z < t$. Equation (4.4) then yields

$$\frac{\partial z}{\partial t} - \frac{y}{t - z}\frac{\partial z}{\partial y} = 0. \tag{4.6}$$

Since the approximations (3.2) and (4.2) are expected to be valid not too far from the tip of the spike, the physically relevant condition for the present analysis is

$$z \ll t. \tag{4.7}$$

General solutions to (4.6) can be addressed by the method of characteristics. For an initial condition $z(y, t_0) \equiv z_0(y) < t_0$, $z(y, t)$ remains constant on the characteristic curves, which then turn out to be given exactly by

$$y = y_0\frac{[t_0 - z_0(y_0)]}{[t - z_0(y_0)]}, \quad z(y, t) = z_0(y_0). \tag{4.8}$$

https://doi.org/10.1017/S0022112004002630 Published online by Cambridge University Press

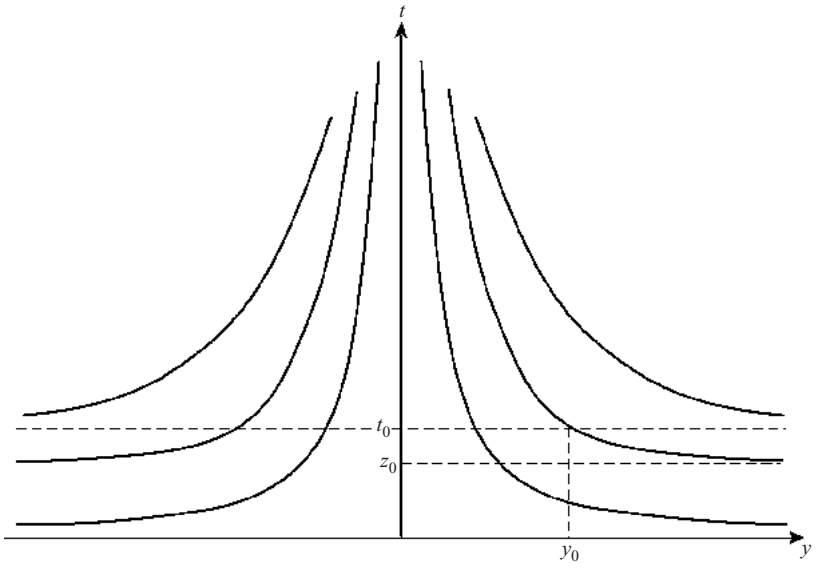


FIGURE 2. (y, t)-diagram for the characteristic base curves from equation (4.8).

Equation (4.8) describes hyperbolas in the (y, t)-diagram for the characteristic base curves, as illustrated in figure 2. These curves do not cross each other in finite time for most functions $z_0(y_0)$; they can cross for $t > t_0$ only if $\mathrm{d}z_0/\mathrm{d}y_0$ becomes sufficiently large in some range of y_0, which is not likely, as discussed more fully in the Appendix B. It follows that typically no singularity appears on the interface for $t \geqslant t_0$ if there is none in the initial condition $z_0(y_0)$. The developments in the present paper are restricted to conditions under which the characteristics base curves do not cross and there are no singularities near the tip.

For $z \ll t$, there is a self-similar solution to (4.6) of the form

$$z(y, t) = \theta(yt), \tag{4.9}$$

where θ is an arbitrary differentiable function. This type of solution can describe the evolution of the curvature of the free surface at the tip of the spike. From equation (4.5), which can be written as $\alpha = (t - z)^2(g/2)$, it can be seen that for small $z(z \ll t)$ the dominant term of $(gt^2/2) - \alpha(y, t)$ is $gtz(y, t)$. The expansion of (4.9) around $y = 0$, namely $z(y, t) \approx (yt)^2\theta''(0)/2$, then shows that the curvature of the spike, $\kappa_s \equiv -\partial^2\alpha/\partial y^2|_{y=0} (\kappa_s > 0)$ increases with time like t^3,

$$\kappa_s \approx gt^3\theta''(0). \tag{4.10}$$

In cylindrical geometry, with y representing the radial distance from the axis of symmetry, a similar approach shows that the equation of the surface near the tip of the spike takes the form $\alpha = gt^2/2 - gt\theta(y\sqrt{t})$ since a factor of 2 then multiplies $\partial z/\partial t$ in (4.6), leading to $z(y, t) = \theta(y\sqrt{t})$ as the self-similar solution; the resulting mean curvature increases with time like t^2,

$$\kappa_s \approx gt^2\theta''(0). \tag{4.11}$$

The value of the constant $\theta''(0)$ must depend on the initial conditions. The present analysis addresses conditions under which $\theta''(0)$ is positive and does not consider possible variations of $\theta''(0)$ with time, which may occur at higher order.

https://doi.org/10.1017/S0022112004002630 Published online by Cambridge University Press

Equation (4.4) possesses formal solutions of the form

$$\alpha^{1/2} = t\sqrt{g/2} + \phi\left(y\alpha^{1/2}\right) \tag{4.12}$$

for any differentiable function ϕ. This implies that, when y is expressed in terms of x and t at the surface, $|y| = \beta(x,t)$, the asymptotic equation for the free surface near the tip of the spike can be written as

$$\beta^2 = \frac{\chi\left(x_s^{1/2} - x^{1/2}\right)}{x} \quad \text{with} \quad x_s(t) = gt^2/2, \tag{4.13}$$

where the function $\chi = (\phi^{-1})^2$ is determined by the initial conditions, ϕ^{-1} here denoting the inverse of the function ϕ.

5. First-order perturbation analysis

In anticipation that the flow is not singular on the symmetry axis $y = 0$, and under the assumption that the flow can be described by analytic functions in the vicinity of the tip, a power series for $f(x,y,t)$ in (3.4) may be introduced in the form

$$f = f_0(x,t) + f_{yy}(x,t)y^2/2 + \ldots \tag{5.1}$$

with

$$f_0(x,t) \ll gx, \quad \partial f_0(x,t)/\partial x \ll g. \tag{5.2}$$

The expansion of equation (3.4) then can be expressed as

$$u = [\sqrt{2gx} + F] + (y^2/2)G + \ldots \tag{5.3}$$

where, $F(x,t) \equiv f_0/\sqrt{2gx}$, $G(x,t) \equiv f_{yy}/\sqrt{2gx}$. The incompressibility condition (2.1) and the symmetry boundary condition that $v = 0$ at $y = 0$ then give

$$v = -[\sqrt{g/2x} + \partial F/\partial x]y - (y^3/3!)\partial G/\partial x + \ldots. \tag{5.4}$$

The second term inside the brackets in (5.3) and (5.4) is smaller than the first in this perturbation analysis. The power series of the velocity potential of (2.4) may be obtained from (5.3) and (5.4) in the form

$$\Phi = -\int^x [\sqrt{2gx'} + F(x',t)]\,\mathrm{d}x' - (y^2/2)\int^x G(x',t)\,\mathrm{d}x' + (y^4/4!)\partial G/\partial x + \ldots \tag{5.5}$$

with the compatibility condition $\int^x G(x',t)\,\mathrm{d}x' = -\sqrt{g/2x} - \partial F/\partial x$, yielding

$$\sqrt{2gx}G = f_{yy} = g/2x - \sqrt{2gx}(\partial^2 F/\partial x^2), \tag{5.6}$$

so that the only unknown that remains in (5.5) is F, equivalent to $f_0(x,t)$ being the only unknown.

According to (5.3), (5.4) and (5.6), in (2.2), (2.3) and (2.5)

$$(u^2+v^2)/2 - gx = \sqrt{2gx}F + \left[(g/x) - \sqrt{2gx}(\partial^2 F/\partial x^2) + \sqrt{2g}(\partial F/\partial x)/x^{1/2}\right]y^2/2 + \ldots, \tag{5.7}$$

where the last two terms inside the brackets are smaller than the first. Use of (5.3), (5.4), (5.6) and (5.7) in (2.2) and (2.3) then readily gives

$$\frac{\partial}{\partial t}F - \left(\frac{y^2}{2}\right)\frac{\partial^2}{\partial x^2}\left(\frac{\partial}{\partial t}F\right) \approx -\frac{\partial}{\partial x}\left[p + \sqrt{2gx}F + \left(\frac{y^2}{2}\right)\frac{g}{x}\right], \tag{5.8}$$

$$-y\frac{\partial}{\partial x}\left(\frac{\partial}{\partial t}F\right) \approx -\frac{\partial}{\partial y}\left[p + \sqrt{2gx}F + \left(\frac{y^2}{2}\right)\frac{g}{x}\right]. \tag{5.9}$$

https://doi.org/10.1017/S0022112004002630 Published online by Cambridge University Press

The pressure may be calculated from these results by first integrating (5.8) from $x = x_s$, where $p = 0$, to an arbitrary value of x, then integrating (5.9) from zero to y at this value of x. The result is

$$p(x, y, t) = \sqrt{2gx_s}F(x_s, t) - \sqrt{2gx}F(x, t) + \int_x^{x_s} (\partial F(x', t)/\partial t)\,\mathrm{d}x' - [g/x - \partial^2 F(x, t)/\partial t\,\partial x](y^2/2) + \ldots. \quad (5.10)$$

If the equation for the free surface is now written as

$$|y| = \beta(x, t), \quad (5.11)$$

then imposing the zero-pressure condition there in (5.10) leads to the equation

$$\sqrt{2gx_s}F(x_s, t) - \sqrt{2gx}F(x, t) + \int_x^{x_s} (\partial F(x', t)/\partial t)\,\mathrm{d}x' = [g/x - \partial^2 F(x, t)/\partial t\partial x]\beta^2/2, \quad (5.12)$$

which is equivalent to the corresponding condition (2.7) that is obtained from the Bernoulli equation (2.5). Equation (5.12) can be viewed as an integrodifferential equation for $f_0(x, t) = \sqrt{2gx}F(x, t)$, given x_s and β, or simply as a partial differential equation for $\int_x^{x_s} F(x', t)\,\mathrm{d}x'$.

The derivative of (5.12) with respect to x evaluated at $x = x_s$, where $\beta = 0$, leads to

$$(\sqrt{2gx_s})\partial f_0/\partial x|_{x=x_s} + \partial f_0/\partial t|_{x=x_s} \approx \left(\sqrt{2}g^{3/2}/\kappa_s x_s^{1/2}\right), \quad (5.13)$$

since $\partial(\beta^2/2)\partial x|_{x=x_s} = -1/\kappa_s$, according to the definition of the curvature, and $(1/\kappa_s)$ $[\partial(\partial F/\partial t)/\partial x]|_{x=x_s}$ is negligible in comparison with $(\partial F/\partial t)_{x=x_s}$ because the characteristic length of variation of $(\partial F/\partial t)_{x=x_s}$ is much larger than $1/\kappa_s$. Equations (2.8) and (5.3) evaluated at $y = 0$ yield the two-term expansion

$$\mathrm{d}x_s/\mathrm{d}t = \sqrt{2gx_s} + [f_0(x_s, t)/\sqrt{2gx_s}] + \ldots, \quad (5.14)$$

which enables (5.13) to be written as

$$\frac{\mathrm{d}}{\mathrm{d}t} f_0(x_s, t) \approx \frac{\sqrt{2}g^{3/2}}{\kappa_s(t)\sqrt{x_s(t)}} + \ldots \quad (5.15)$$

at leading order, since the last term in (5.14) is small. Equation (5.15) confirms that the perturbation parameter $|f(x_s, 0, t)|/(gx_s)$ is small in the long-time limit.

Equations (5.14) and (5.15) describe how the acceleration of the spike approaches g. The time derivative of (5.14) can be written in a two-term expansion as

$$\frac{\mathrm{d}^2 x_s}{\mathrm{d}t^2} = g + \frac{\mathrm{d}f_0/\mathrm{d}t}{\mathrm{d}x_s/\mathrm{d}t}, \quad (5.16)$$

and (5.15) may be substituted into this expression to show, using (3.3) and (4.10), that

$$\frac{\mathrm{d}^2 x_s}{\mathrm{d}t^2} - g \approx \frac{2}{g\theta''(0)t^5}. \quad (5.17)$$

A similar analysis in cylindrical geometry, which requires using (4.11) instead of (4.10), leads to

$$\frac{\mathrm{d}^2 x_s}{\mathrm{d}t^2} - g = \frac{3}{2g\theta''(0)t^4}. \quad (5.18)$$

https://doi.org/10.1017/S0022112004002630 Published online by Cambridge University Press

The result in (5.15) shows from (3.3) and (4.10) that $\mathrm{d}f_0/\mathrm{d}t$ is proportional to $1/t^4$ for large time, so that according to (3.3), (3.4) and (5.14), the basic assumptions in (3.5) are self-consistent, provided that the order of magnitude of each term on the left-hand side of (5.13) is not larger than the right-hand side. The approach to free fall is seen from (5.17) and (5.18) to occur from above, that is, the acceleration of the tip must always overshoot then approach free fall from above.

6. Discussion of the results

Based on the assumption that the asymptotic flow field near the tip of the spike is close to that imposed by free fall, power laws in time for the evolution at long time of the curvature and of the acceleration of the tip have been obtained here. A self-similar equation for the shape of the free surface near the tip also has been derived. It has been established that, in the long-time limit, no singularity can appear at a finite time near the tip unless the initial conditions are unusual in the sense that they possess singularities or exhibit an excessively steep interface far from the tip. Although formation of finite-time singularities may be possible at intermediate time and away from the tip, that appears not very likely for periodic and symmetric initial conditions, as is being confirmed by accurate direct numerical simulations, the most recent by L. Duchemin & C. Josserand (2004, personal communication), based on an integral method. None of the results presented here are compatible with a single-mode Fourier-decomposition approximation, which works so well for the bubble. The failure of this approach for the spike is associated with the free-fall spatial dependence of the flow.

Appendix A. Relationship to inertial-confinement instabilities

The study is motivated by the hydrodynamic instabilities of ablation fronts in inertial-confinement fusion. There are two reasons for potential relevance to this problem. First, the acceleration is very strong (Froude number of order unity) and the density jump across the ablation front is very large (Atwood number close to unity), so that the ablation, as studied by the model of Clavin & Masse (2004), is, in a sense, a weak perturbation to this Rayleigh–Taylor instability. Second, as in flames (see for example the book of Williams (1985), and the review paper of Clavin (2000)), the ablation introduces a constraint, imposing conservation of the tangential flow velocity component across the front, so that the secondary instability of the Kelvin–Helmholtz type, leading to the 'roll-up' or 'mushroom' structures observed in Rayleigh–Taylor instability for non-unity Atwood number, will tend to be suppressed, as it is for unity Atwood number.

Appendix B. Possibilities for development of singularities

Finite-time singularities in the flow will arise if the characteristic base curves defined by equation (4.8) cross for $t > t_0$. This depends on the function $z_0(y_0)$ which must be non-decreasing with increasing $|y_0|$ but remain less than t_0. By considering two different characteristic curves, one with the initial value $y_{01} > 0$ and the other with the initial value $y_{02} > y_{01}$, it can be shown that these two characteristics cross only if

$$[y_{02}z_0(y_{02}) - y_{01}z_0(y_{01})]/t_0 \geqslant y_{02} - y_{01}. \tag{B 1}$$

From this it follows that, if y_{01} and y_{02} are sufficiently close together, then the condition that must be satisfied for the characteristic curves not to cross is

$$\mathrm{d}(y_0z_0)/\mathrm{d}y_0 < t_0 \tag{B 2}$$

https://doi.org/10.1017/S0022112004002630 Published online by Cambridge University Press

for all y_0, with the given initial profile $z_0(y_0)$. This condition is also sufficient in the range of the present analysis, $z_0 \ll t_0$.

Equation (B2) is always satisfied on the plane or axis of symmetry, $y_0 = 0$, because of the requirement that $z_0 < t_0$. Therefore if characteristic curves do cross, leading to a singularity, that event must occur away from the tip of the spike, on its side. It can be seen by an example that in the range of validity of the analysis in this paper, which is an expansion about the tip for large time, (B2) is satisfied. Suppose that $z_0(y_0)$ is parabolic, say $z_0 = cy_0^2$, with c a constant. Then (B2) requires $3cy_0^2 < t_0$, which is $3z_0 < t_0$, a condition that is satisfied by the requirement $z_0 \ll t_0$ of the analysis.

Equation (B2) is satisfied by the initial conditions of the original problem, $z_0(y_0) = 0$, with $t_0 = 0$, and the small-time development will not change that, but evolution at intermediate times could violate (B2). Beyond the range of validity of the perturbation analysis, computations suggest that the tail of the spike becomes essentially straight, $z_0 = b(y_0 - a)$, where a and b are constant, a being of the order of the radius of curvature of the tip. In this case (B2) is $b(2y_0 - a) = 2z_0 + ab < t_0$, which can be violated only if ab is sufficiently large. Part of the sides of the spike initially must be very steep for a singularity to develop, which is difficult to achieve in view of the general requirement that $z_0 < t_0$. If for particular initial conditions finite-time singularities were to develop, they could conceivably propagate to $y = 0$ and thereby override the present analysis.

This work was supported by CEA/DIP through grant 4600051147/P6H29 and by HSF through grant CTS0129562.

REFERENCES

Abarzhi, S. 1998 Steady state flows in Rayleigh–Taylor instability. *Phys. Rev. Lett.* **81**, 337–340.

Abarzhi, S., Nishihihara, K. & Glimm, J. 2003 Rayleigh–Taylor instabilities for fluids with a finite density ratio. *Phys. Lett.* A **317**, 470–476.

Baker, G. & Beale, J. 2004 Vortex blob methods applied to interfacial motion. *J. Comput. Phys.* **196**, 233–258.

Clavin, P. 2000 Dynamics of combustion fronts in premixed gases: from flames to detonations. *Proc. Comb. Inst.* **28**, 569–585.

Clavin, P. & Masse, L. 2004 Instabilities of ablation fronts in inertial confinement fusion: a comparison with flames. *Phys. Plasmas* **11**, 690–705.

Duchemin, L. & Josserand, C. 2004 Private communication.

Goncharov, V. 2002 Analytical model of nonlinear, single-mode classical Rayleigh–Taylor instability at arbitrary Atwood numbers. *Phys. Rev. Lett.* **88**, 134052-1–134052-4.

Inogamov, N. 1999 The role of Rayleigh-Taylor and Richtmyer-Meshkov instabilities in astrophysics: an introduction. *Astrophys. Space Phys.* **10**, 1–335.

Kull, H. 1991 Theory of the Rayleigh–Taylor instability. *Phys. Rep.* **206**, 197–325.

Layzer, D. 1955 On the instability of superimposed fluids in a gravitational field. *Astrophys. J.* **122**, 1–12.

Mikaelian, K. 1998 Analytic approach to nonlinear Rayleigh–Taylor and Richtmyer–Meshkov instabilities. *Phys. Rev. Lett.* **80**, 508–511.

Rayleigh, Lord 1900 *Scientific Papers*. Cambridge University Press, Vol. II, 200–207.

Tanveer, S. 1993 Singularities in the classical Rayleigh–Taylor flow: formation and subsequent motion. *Proc. R. Soc. Lond.* A **441**, 501–525.

Taylor, G. 1950 The instability of liquid surfaces when accelerated in a direction perpendicular to their planes. *Proc. R. Soc. Lond.* A **201**, 192–196.

Williams, F. 1985 *Combustion Theory*, 2nd edn. Addison-Wesley.

Yoshikawa, T. & Balk, A. 2003 A conformal-mapping model for bubbles and fingers of the Rayleigh–Taylor instability. *Math. Comput. Modelling* **38**, 113–121.

Zhang, Q. 1998 Analytical solutions of Layzer-type approach to unstable interfacial fluid mixing. *Phys. Rev. Lett.* **81**, 3391–3394.

https://doi.org/10.1017/S0022112004002630 Published online by Cambridge University Press